Atom Detection and Photon Production in a Scalable, Open, Optical Microcavity

M. Trupke, J. Goldwin, B. Darquié, G. Dutier,* S. Eriksson, J. Ashmore, and E. A. Hinds

Centre for Cold Matter, Imperial College, Prince Consort Road, London SW7 2BW, United Kingdom

(Received 23 April 2007; published 8 August 2007)

A microfabricated Fabry-Perot optical resonator has been used for atom detection and photon production with less than 1 atom on average in the cavity mode. Our cavity design combines the intrinsic scalability of microfabrication processes with direct coupling of the cavity field to single-mode optical waveguides or fibers. The presence of the atom is seen through changes in both the intensity and the noise characteristics of probe light reflected from the cavity input mirror. An excitation laser passing transversely through the cavity triggers photon emission into the cavity mode and hence into the single-mode fiber. These are first steps toward building an optical microcavity network on an atom chip for applications in quantum information processing.

DOI: 10.1103/PhysRevLett.99.063601 PACS numbers: 42.50.Pq, 03.67.−a, 32.80.Pj, 42.81.Qb

When a neutral atom is placed in a high-finesse optical cavity, the electric dipole coupling between the atom and the light field can lead to quantum coherence between the two. This fact forms the basis of cavity quantum electrodynamics (QED) [1]. Recently, there has been considerable interest in the possibility of applying cavity QED to problems in quantum information processing, as reviewed, for example, in Ref. [2]. Single photons have been generated on demand from falling [3] and trapped [4] atoms in high-finesse Fabry-Perot cavities, and recent experiments have investigated the cavity-assisted generation of single photons from atomic ensembles [5]. These are important steps toward building multiple-cavity quantum information networks, such as those proposed in Ref. [6]. However, experiments so far have been limited to single cavities by the technical demands of achieving high enough finesse. Outstanding challenges now are to make the cavities smaller, to fabricate them in large numbers with the possibility of multiple interconnects, and to load them conveniently and deterministically with atoms. This would pave the way to circuit-model quantum computers [7], to one-way computations based on cluster states [8], and to other schemes requiring multiple cavities [9].

As a first move in this direction, two recent experiments have used a small magnetic guide to load atoms into a cavity [10]. However, the cavities in these experiments were 2–3 cm long and therefore not more scalable than a conventional Fabry-Perot cavity. By contrast, Aoki *et al.* have dropped atoms close to a microscopic toroidal cavity and observed evidence of strong coupling [11]. These resonators can be microfabricated in large arrays; however, they are not easily used for controlled atom-cavity coupling because of the need to position the atom very precisely in the evanescent field just outside the surface of the resonator. For this reason it is of interest to consider microscopic Fabry-Perot cavities, whose open structure gives access to the central part of the cavity field. In one recent design [12], the two mirrors of such a resonator are formed by optical fibers whose tips have been modified into concave reflectors. This design can achieve small mode volumes and can collect the light efficiently, but is not easily scaled.

In collaboration with the group of Kraft, we have developed a unique resonator design using curved micromirrors fabricated at desired positions on a silicon wafer [13,14]. The cavities are closed by plane mirrors on the ends of optical fibers or waveguides. This design combines the intrinsic scalability of microfabrication processes with direct coupling of the cavity field to single-mode optical waveguides or fibers. Advances in the production of etched waveguides [15] and plane-ended fiber arrays, together with the recent production of etched three-dimensional actuators [16], promise to make these cavities fully integrated and scalable. Here we report on the first use of such cavities to detect atoms and produce photons. We study the reflection spectrum and noise characteristics of the coupled atom-cavity system and we trigger the cavity-enhanced emission of a few photons from the atoms into the fiber. These are all essential steps toward integrating the cavities on an atom chip for quantum information processing.

The paraxial TEM00 cavity mode with wave number k has an intensity distribution given by $D(\rho, z) = (w_0/w)^2 \sin^2(kz) \exp(-2\rho^2/w^2)$, where w characterizes the transverse size of the mode, w_0 is its minimum value, and ρ, z are the cylindrical coordinates. The integral of this distribution over a cavity of length L gives the mode volume $V = \pi w_0^2 L/4$, and the weighted sum over the positions of the atoms $\sum_j D(\rho_j, z_j) \equiv N$ defines the effective number of atoms in the cavity. For an atom placed at the maximum of D, the coherent atom-cavity coupling is characterized by $g_0 = \mu\sqrt{\omega_C/(2\hbar\varepsilon_0 V)}$, where μ is the electric dipole transition moment, ω_C is the angular frequency of the mode, and ε_0 is the free-space permittivity. Our microfabricated cavities give large values of g_0 by virtue of their extremely small mode volume. For example, the experiments described here use a cavity with $L = 130\ \mu$m and $w_0 = 4.6\ \mu$m. This gives $g_0 = 6.1 \times 10^8\ \text{s}^{-1}$ for $\sigma^{\pm}$-polarized light driving the cycling transi-

tion $|F = 3, M = \pm 3\rangle \rightarrow |F' = 4, M' = \pm 4\rangle$ of the D_2 line in ^{85}Rb, which is used in this work. This rate is equal to half the single-photon Rabi frequency. It is to be compared with $\gamma = 1.9 \times 10^7$ s^{-1} [17], which is half the natural decay rate of the excited atomic population and with κ, which is half the decay rate of power in the cavity. The rate κ is related to the cavity finesse $\mathcal{F}$ by $\kappa = \pi c/(2L\mathcal{F})$ (c is the speed of light), and hence to the reflectivities of the mirrors [18]. Although we have previously made microcavities with finesse $\mathcal{F} > 5000$ [13], these first experiments with atoms use $\mathcal{F} = 280$, corresponding to $\kappa = 1.3 \times 10^{10}$ s^{-1}. From these three rates, one can construct the dimensionless parameter $\kappa\gamma/g_0^2$, which is the number of atoms needed to modify the cavity field appreciably [1,19]. This has the value 0.7 for this work, indicating that a single atom is enough to significantly effect the cavity field.

The apparatus is shown in Fig. 1. Two fibers with plane dielectric mirrors on their ends are held in parallel grooves 2 mm apart on a glass-ceramic substrate. The fibers face two of an array of concave mirrors etched into a silicon wafer on a 500 μm square grid. These mirrors have a 186 μm radius of curvature and 100 μm diameter, and they are coated with a dielectric multilayer to reflect light at 780 nm. The silicon mirror chip is mounted on a translator (PZT), which is adjusted every 100 ms under computer control to tune the upper cavity to the free-space atomic resonance. Both cavities can be run simultaneously, but in this work the lower cavity was not used. A mirror is used to form a magneto-optical trap (MOT) 6 mm above the active cavity, where up to 4×10^7 cold ^{85}Rb atoms are collected. The magnetic quadrupole field of the MOT is switched off and optical molasses [20] cools the cloud over 15 ms to ~30 μK. The light is then shut off, allowing the atoms to fall into the microcavity through a 1 mm hole in the mirror. Weak probe light (typically ~1 pW) is incident on the upper cavity through a beam splitter and the reflected photons are counted in 10 μs bins by a Perkin Elmer SPCM-AQR-14 avalanche photodiode (APD) to detect the presence or absence of atoms. For the experiment presented in Fig. 1, probe light reflected from the cavity input mirror produces an APD count rate far from resonance of $I_0 = 419 \times 10^3$ s^{-1}. At resonance, this drops to $I_1 = 272 \times 10^3$ s^{-1} through interference with the field returning from within the cavity via the input mirror. This is the base level of the graph in Fig. 1. With the arrival of atoms, the count rate rises to a peak of $I_2 = 315 \times 10^3$ s^{-1} because the field in the cavity, and hence the field leaking back out through the input mirror, is reduced by the presence of the atoms. At resonance, the ratio of intracavity fields with no atoms and with N atoms is just $(\sqrt{I_0} - \sqrt{I_1})/(\sqrt{I_0} - \sqrt{I_2})$, which equates to $(1 + Ng^2/\kappa\gamma)$ [1]. Since the Zeeman sublevels are mixed in the optical molasses, we take $g^2 = (3/7)g_0^2$, where the factor of 3/7 averages over all the $F = 3$ sublevels. The solid curve in Fig. 1 is a fit to this model for a cloud with Gaussian density distribution, which gives $N = 0.7$ at the peak. We expect this result to be a slight underestimate because the number of atoms is randomly fluctuating and the reflected power is a nonlinear function of that number, saturating at higher values. Nevertheless, it shows that $N \simeq 1$, in agreement with our knowledge of the initial atom number and temperature in the MOT.

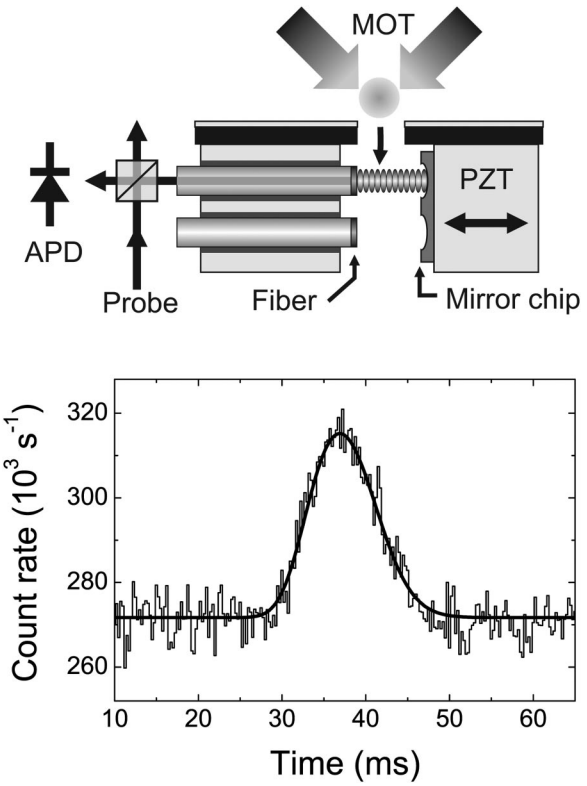

FIG. 1. Apparatus (not to scale). Graph: change in reflected probe light as atoms traverse the cavity. Averaging window: 250 μs. Laser, cavity, and atom frequencies are equal: $\omega_L = \omega_C = \omega_A$. Atoms are released from optical molasses at time $t = 0$, and 34 identical drops are averaged. There are ~0.7 atoms in the cavity on average at the peak.

For a more detailed study, we have measured the fraction of power reflected at the atom peak I_2/I_0 as a function of the probe laser frequency ω_L, keeping the cavity frequency ω_C centered on the atomic resonance frequency ω_A. The data points in Fig. 2 show the result of this scan for two different values of the initial atom number in the MOT. The solid lines are a fit to the functional dependence [21,22]

$$\frac{I_2}{I_0} = \frac{[1 + \frac{Ng^2/(\kappa\gamma)}{1+(\Delta/\gamma)^2} - \beta]^2 + (\frac{\Delta}{\kappa})^2[1 - \frac{N(g/\gamma)^2}{1+(\Delta/\gamma)^2}]^2}{[1 + \frac{Ng^2/(\kappa\gamma)}{1+(\Delta/\gamma)^2}]^2 + (\frac{\Delta}{\kappa})^2[1 - \frac{N(g/\gamma)^2}{1+(\Delta/\gamma)^2}]^2}, \quad (1)$$

where $\Delta = \omega_L - \omega_{C,A}$ is the probe laser detuning. The parameter β characterizes the maximum fringe contrast, and can be determined from the response of the resonant empty cavity, according to $I_1/I_0 = (1 - \beta)^2$. For our pa-

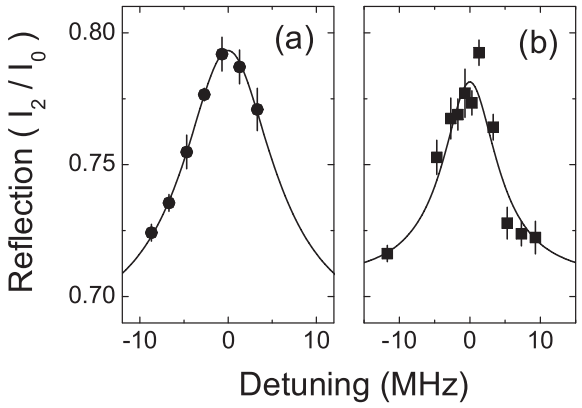

FIG. 2. Peak probe laser reflection with $\omega_C = \omega_A$ versus detuning $(\omega_L - \omega_A)/2\pi$ for different initial MOT numbers. (a) $\langle N \rangle = 1.1$ atoms in the cavity; full-width at half-maximum $2.1 \times 2\gamma$. (b) $\langle N \rangle = 0.6$; width $1.7 \times 2\gamma$. Solid curves are Monte Carlo fits to the data using Eq. (1).

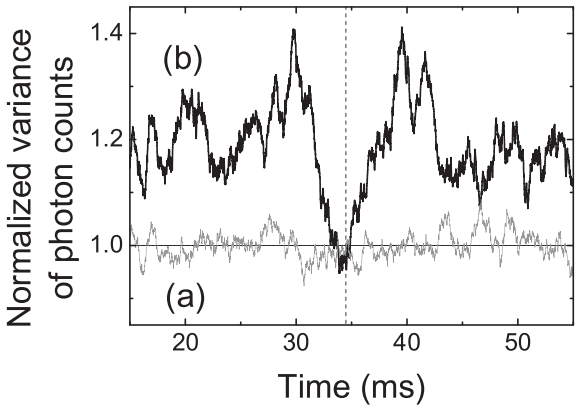

FIG. 3. Normalized variance of the photon counts reflected from the cavity as a function of time, determined from 48 drops. (a) Nonresonant cavity. (b) Resonant cavity. Horizontal line: shot-noise limit. Vertical dashed line: arrival time of the peak number of atoms.

rameters, Eq. (1) describes a spectrum whose peak and width both increase with N. In order to account for number fluctuations, we fit this formula to the data using a Monte Carlo simulation, similar to that of Ref. [22], but with two additions. First, because our Rayleigh length $z_R = w_0^2/(2k)$ is comparable to the cavity length, we include in our model the variation of the transverse mode size $w = w_0\sqrt{1 + (z/z_R)^2}$. Second, we convolve the calculated spectra with a Lorentzian to account for the measured linewidth of our probe laser, which is 1.2 MHz. The Monte Carlo fits shown in Figs. 2(a) and 2(b) yield average atom numbers of $\langle N \rangle = 1.1$ and 0.64, with spectral widths of $2.1 \times 2\gamma$ and $1.7 \times 2\gamma$, respectively. This result demonstrates that our microcavities can measure very small atom numbers, even at such modest finesse.

Another way to detect the arrival of atoms in the cavity is through the photon statistics. Therefore, we performed 48 drops of the atom cloud, recording the APD signal versus time as a series of counts m, each being the integral of the rate over a time interval $\tau = 10\ \mu$s. These counts were corrected [23] for the measured dead time of the detector $\tau_d = 44$ ns according to $n = m/(1 - m\tau_d/\tau)$. The normalized variance of the counts $f(n) \equiv \mathrm{Var}(n)/\langle n \rangle$ was then corrected [24] for the 90% beam splitter transmission and the 60% APD quantum efficiency according to $f_{\mathrm{corr}}(n) - 1 = 0.54[f(n) - 1]$ in order to derive the normalized variance of the photon numbers shown in Fig. 3. With the cavity far from resonance and in the absence of atoms [curve (a)], this is close to unity, as expected for statistical noise. However, on resonance [curve (b)], there is additional technical noise due to vibrations of the cavity length. This curve has audio-frequency fluctuations, which are also seen as distinct peaks in the Fourier spectrum of the noise recorded over longer time intervals. The excess noise is suppressed by the arrival of the atoms at a time $t \sim 35$ ms. In part this is because the reflection minimum is less sensitive to variations of cavity length when the atoms are present. This suppression mechanism accounts for only half the noise reduction we observe. The additional noise reduction is of unknown origin, but may be quantum mechanical [25]. This will require further investigation after the stability of the upper cavity length has been improved using active stabilization of the lower cavity (Fig. 1) during the atom drop.

The radiation pattern of an atom excited in the cavity is strongly enhanced in the direction of the cavity mode, a phenomenon known as the Purcell effect [19]. Thus the cavity enhances the emission of photons into the single-mode fiber attached to the plane mirror. Without a cavity, only about 0.01% of the fluorescence photons would radiate into the fiber. By contrast, for our parameters, the rate of emission into the cavity $2g^2/\kappa$ is roughly equal to the free-space rate 2γ. In order to demonstrate this effect in our microcavities, we prepare and drop an atom cloud as described above, monitoring the reflection of the weak probe laser to determine when the atom number is at its peak value of $N \simeq 1$. At this point we turn on a resonant laser beam (40 mW/cm^2) propagating transverse to the cavity axis, in order to excite the atoms. As shown in Fig. 4(a), the reflection signal recorded on the APD drops abruptly when the excitation laser is turned on. This is due to a combination of optical pumping into the dark $F = 2$ state and physical removal of the atoms from the cavity as a result of the radiation pressure. The experiment is repeated without the probe laser, but under otherwise identical conditions, so that the cavity-stimulated photons can be detected using the APD. As shown in Fig. 4(b), we see a burst of fluorescence at the moment of excitation. This is absent if there are no atoms in the cavity or if the cavity is detuned from resonance, confirming that the detected light is indeed due to the Purcell-enhanced transfer of photons from the excitation laser beam into the fiber via both the atoms and

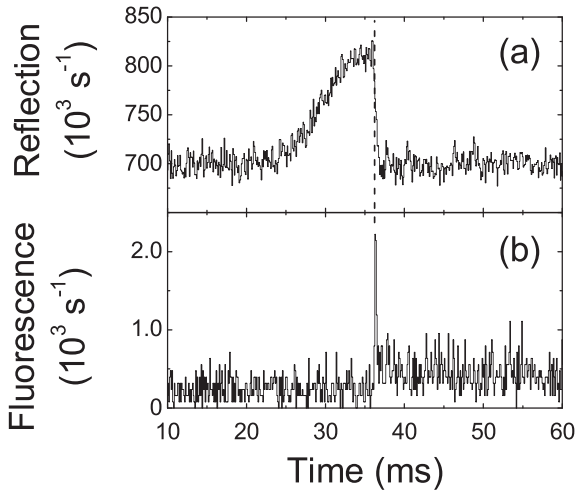

FIG. 4. (a) Probe reflection signal showing abrupt atom loss when the excitation laser is turned on. (b) Cavity-stimulated decay generates a pulse of photons in the fiber when the atom cloud is excited. The dotted line shows coincidence of the photon pulse with the turn-on of the excitation laser.

cavity. Typically we detect one or two photons in the peak, which is consistent with the prediction of a master equation model, taking into account cavity-enhanced optical pumping into the dark $F = 2$ state and the number of atoms known from Fig. 4(a). The efficiency of excitation transfer from the atom to the cavity is limited at present by the 50% of photons radiated out of the cavity, but with the higher-quality $\mathcal{F} > 5000$ cavities available in our laboratory, we anticipate reaching over 92% in future experiments. This would make our chip cavity a useful source of photons on demand and the entanglement between the atom and the photon in the fiber would be a useful resource for quantum information processing.

In conclusion, we have used a microfabricated optical cavity based on a silicon wafer to detect less than one atom on average with a signal/noise ratio of 3 over ~ 250 μs. In the next experiment this cavity will be rebuilt to give a much improved fringe visibility and hence a reduced detection time of ~ 2 μs, allowing us to follow a given single atom during the ~ 15 μs it takes to fall through the cavity. Our cavity design results in a large single-photon Rabi frequency, and cavity photons are conveniently coupled to a single-mode optical fiber or waveguide, which is integral to the construction. Cold atoms falling through a cavity were detected by their effect on the cavity reflection spectrum and by their influence on the noise in the reflected light. We also triggered the emission of photons into the fiber by means of the Purcell effect. These results constitute first steps toward building an optical microcavity network on a chip for applications in quantum information processing.

This work was supported by EU networks Atom Chips, Conquest, and SCALA, by the Royal Society, and by EPSRC grants for QIPIRC, CCM programme and Basic Technology. The group of M. Kraft at Southampton University etched the silicon mirrors.

*Present address: UMR 7538 du CNRS, Université Paris 13, 99 Avenue J.-B. Clément, 93430 Villetaneuse, France.

[1] *Cavity Quantum Electrodynamics*, edited by P. R. Berman (Academic Press, San Diego, 1994).
[2] S. J. van Enk, H. J. Kimble, and H. Mabuchi, Quant. Info. Proc. **3**, 75 (2004).
[3] A. Kuhn, M. Hennrich, and G. Rempe, Phys. Rev. Lett. **89**, 067901 (2002).
[4] J. McKeever *et al.*, Science **303**, 1992 (2004); M. Hijlkema *et al.*, Nature Phys. **3**, 253 (2007).
[5] A. T. Black, J. K. Thompson, and V. Vuletić, Phys. Rev. Lett. **95**, 133601 (2005); A. T. Black, J. K. Thompson, and V. Vuletić, Science **313**, 74 (2006).
[6] J. I. Cirac, P. Zoller, H. J. Kimble, and H. Mabuchi, Phys. Rev. Lett. **78**, 3221 (1997).
[7] D. P. DiVincenzo, Fortschr. Phys. **48**, 771 (2000).
[8] R. Raussendorf and H. J. Briegel, Phys. Rev. Lett. **86**, 5188 (2001).
[9] L. M. Duan and H. J. Kimble, Phys. Rev. Lett. **90**, 253601 (2003); D. E. Browne, M. B. Plenio, and S. F. Huelga, *ibid.* **91**, 067901 (2003); S. Clark, A. Peng, M. Gu, and S. Parkins, *ibid.* **91**, 177901 (2003); M. J. Hartmann, F. G. S. L. Brandao, and M. B. Plenio, Nature Phys. **2**, 849 (2006); A. D. Greentree, C. Tahan, J. H. Cole, and L. L. C. Hollenberg, *ibid.* **2**, 856 (2006); A. Serafini, S. Mancini, and S. Bose, Phys. Rev. Lett. **96**, 010503 (2006); Z. Yin and F. Li, Phys. Rev. A **75**, 012324 (2007).
[10] I. Teper, Y.-J. Lin, and V. Vuletić, Phys. Rev. Lett. **97**, 023002 (2006); A. Haase, B. Hessmo, and J. Schmiedmayer, Opt. Lett. **31**, 268 (2006).
[11] T. Aoki *et al.*, Nature (London) **443**, 671 (2006).
[12] T. Steinmetz *et al.*, Appl. Phys. Lett. **89**, 111110 (2006).
[13] M. Trupke *et al.*, Appl. Phys. Lett. **87**, 211106 (2005).
[14] S. Eriksson *et al.*, Eur. Phys. J. D **35**, 135 (2005).
[15] See, for example, A. A. Bettiol *et al.*, Nucl. Instrum. Methods Phys. Res., Sect. B **231**, 364 (2005).
[16] C. O. Gollasch *et al.*, J. Micromech. Microeng. **15**, S39 (2005).
[17] U. Volz and H. Schmoranzer, Phys. Scr. **T65**, 48 (1996).
[18] B. E. A. Saleh and M. C. Teich, *Fundamentals of Photonics* (John Wiley & Sons, New York, 1991).
[19] E. M. Purcell, Phys. Rev. **69**, 674 (1946); D. Kleppner, Phys. Rev. Lett. **47**, 233 (1981).
[20] P. D. Lett *et al.*, Phys. Rev. Lett. **61**, 169 (1988).
[21] P. Horak *et al.*, Phys. Rev. A **67**, 043806 (2003).
[22] R. J. Thompson, G. Rempe, and H. J. Kimble, Phys. Rev. Lett. **68**, 1132 (1992).
[23] See, for example, D. F. Yu and J. A. Fessler, Phys. Med. Biol. **45**, 2043 (2000).
[24] H.-A. Bachor and T. C. Ralph, *A Guide to Experiments in Quantum Optics* (Wiley VCH, Weinheim, 2004).
[25] G. Rempe *et al.*, Phys. Rev. Lett. **67**, 1727 (1991); see also H. J. Carmichael *et al.*, Opt. Commun. **82**, 73 (1991).